International Journal of Applied Mathematics

Volume 36 No. 2 2023, 171-187
ISSN: 1311-1728 (printed version); ISSN: 1314-8060 (on-line version)
doi: http://dx.doi.org/10.12732/ijam.v36i2.3

MODELING AND SIMULATION OF THE IMPACT OF RAINFALL ON DRIVING VEHICLES

Raj Kumar Pradhan[1,2 §], Samir Shrestha[1],
Dil Bahadur Gurung[1]

[1] Department of Mathematics, School of Science
Kathmandu University, Dhulikhel - 45210, NEPAL
[2]Department of Mathematics, Khwopa College, Dekocha
Bhaktapur - 44800, NEPAL

Abstract: Driving vehicles are impacted significantly by several environmental factors like rainfall, snowfall, storm, etc. Drivers attempt to adapt to the new environment by altering their driving behavior. In this paper, a new model equation of the dynamic equation of traffic flow under the consideration of different optimal velocities by incorporating the impact of rainfall on driving vehicles is proposed. The impact of rainfall is taken as the rainfall-resisting force on the vehicle proportional to the velocity of the driving vehicle. The parabolic impact of rainfall is studied on the driving vehicles that start at the green traffic signal at the intersection of the road. The dynamical behavior such as acceleration, velocity, and spacing between the consecutive vehicles of different car-following models are studied through the numerical simulation using the proposed model.

AMS Subject Classification: 37M06, 62P35, 65L12, 74H15, 93A30
Key Words: traffic flow; optimal velocity; rainfall; dynamical behavior; car-following models

1. Introduction

The car-following model describes the relationship between the following and the leading vehicles by stating that every individual vehicle always accelerates or

Received: February 21, 2023

[§]Correspondence author

decelerates in response to the stimulus surrounding it. Therefore, the equation of motion of i^{th} vehicle depends on the response to its stimulus. The motion of i^{th} vehicle can be summarized by the equation:

$$[\text{Response}]_i \propto [\text{Stimulus}]_i \, .$$

The model types differ depending on how the stimulus is defined. However, in general, the stimulus may include the vehicle's velocity, relative velocity, acceleration, and the spacing between the following vehicle (i^{th} vehicle) and the leading vehicle ($(i-1)^{th}$ vehicle).

The car-following model was first introduced in 1953 by Pipes [11], without taking into account the impact of the spacing between the vehicles and any extra knowledge on the car-following behavior, the author had just taken into account the relative velocities of the vehicles. Due to the inconsistency with the actual situation, Bando et al. [1] proposed a car-following model, so-called Optimal Velocity (OV) model in 1995. This model had accounted the influence of spacing between the consecutive vehicles on the speed of the follower vehicle. The researchers indicated that each driver of a vehicle has an optimal velocity that depends on the distance between it and the vehicle in front of it. Helbing and Tilch [6] in 1998, noticed that when the data of traffic trajectory was applied to calibrate the optimal velocity function, unrealistic deceleration and an impractically too high acceleration occurred in the optimal velocity model. So, the authors proposed a model, called Generalized Force (GF) model [6] to overcome the deficiency of the optimal velocity car-following model. Wilson [17] explained how to obtain the speed-headway function and how to analyze the solutions for a uniform flow's linear stability. Additionally, he displayed the simulation results, which demonstrated the solution behavior under an unstable uniform flow. A brand-new car-following model known as the Full Velocity Difference (FVD) model was developed by Jiang et al. [7] in 2001. The positive and negative velocity differences were considered in this model. According to their research, both positive and negative speed variances will have an effect on the car that follows. In a real-world problem, the following vehicle may respond to the variation of the nearest preceding vehicle. It is also to be considered with the multiple preceding vehicles. Therefore, drivers of the following vehicles can receive information about other vehicles on the road by applying the Intelligent Transportation System (ITS), and they can determine the velocity of their own vehicle. On the basis of this concepts, Ge et al. [4] proposed an extended car-following model. Similar to this, Wang et al. [16] developed a novel car-following model known as the multiple velocity difference (MVD) model that takes into account the stimulus from several preceding vehicles. The numerical analyses reveal that the critical value of the sensitivity in the MVD model reduces when compared to the FVD model. It is also noted that the stable region is apparently enlarged.

Previous research has shown that velocity or headway differences can help to stabilize traffic flow. They considered either the velocity difference or headway difference of the leading vehicles. By implementing both strategies, it is anticipated that the traffic flow will become more steady. On the basis of this idea, an extended car-following model is proposed by Xie et al. [18], called the "multiple headway and velocity difference model", that includes both the velocity and the difference of multiple preceding vehicles. Sun et al. [2] proposed another way of velocity difference and multiple headway model considering the acceleration difference of multiple preceding vehicles.

An intelligent transportation system-based on two-velocity-difference model was put forth by Ge et al. [3] by accounting for the relative velocities of leading and following on a single-lane roadway. They expanded a car-following model and came up with the Two Velocity Difference (TVD) model. They upgraded FVD models taking into account different factors influencing the driver to determine the optimal speed. Gong et al. [5] suggested a novel full velocity difference car-following model based on the FVD model that takes into account the imbalance of the vehicle's deceleration and acceleration processes. The researchers in literature [13, 15] put forward a car-following model based on a calibrated speed-headway function that took into account vehicle communication and road conditions. The researchers in the literature [14] improved the FVD model's parameters by adding a new component to create an extended model. They examined how information about a disturbance downstream affected the car-following behavior. According to Tang et al. [12], the optimal velocity of the following vehicle is connected to both the precise spacing of the vehicle and the perceived spacing of the vehicle by the driver of the following vehicle. The optimal velocity function (OVF), on which the optimal velocity car-following model is based, has been extensively studied in research in order to determine how the optimal velocity affects car-following behavior [8, 10]. Jiao et al. [9] introduced an extended car-following model that takes into account the drivers' attributes as part of vehicle-to-vehicle communication. The vehicle and the driver are significantly impacted by several environmental factors. The connection between pavement and vehicles is impacted by unfavorable weather conditions. Drivers attempt to adapt to the new environment by altering their driving style. The magnitude and the intensity of the event can have a significant impact on traffic and road safety characteristics. Numerous studies have examined how rain affects traffic, accident risk, and variations in transportation demand.

Rainfall has the greatest impact on traffic flow among weather events because of the following factors: (i) reduced visibility (ii) decreased coefficient of adhesion between the road surface and the vehicle and (iii) greater risk of aquaplaning. In these situations, drivers slow down their speed and increase their headway, slowing traffic flow and increasing travel time. The speed-density functions that represent the process of continuous traffic flow are changing as a result of the speed reduction, and the stable-unstable domain is shifting.

In this paper, we propose a model of the dynamic equation of traffic flow and present the dynamical behavior of the different car-following models introducing the impact of rainfall. The paper continues with different car-following models depending on optimal velocity, drivers' characteristics and relative velocity in Section 2 followed by numerical simulations and implementation of proposed model with discussion in Section 3. Finally, Section 4 presents the conclusion of the study.

2. Car-following Models

The single-lane car-following model can be modeled as

$$\frac{dv_i}{dt} = f(v_i,\, \Delta x_i,\, \Delta v_i,\, \cdots), \tag{1}$$

where v_i, Δx_i, Δv_i are the speed of i^{th} vehicle, headway and relative speed respectively; f is the stimulus function of i^{th} vehicle. The schematic diagram of the car-following model is shown in Figure 1.

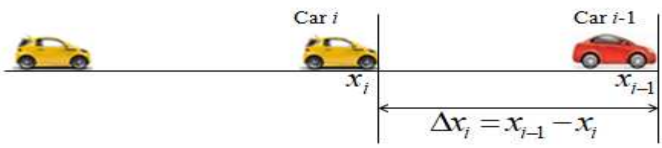

Figure 1: Schematic diagram of car-following model.

2.1. Models Discussion

The Optimal Velocity (OV) model is a traffic flow model introduced by Bando et al. [1]. They defined governing equation as

$$\frac{dx_i}{dt} \;=\; v_i, \tag{2}$$

$$\frac{dv_i}{dt} = \kappa\{V(\Delta x) - v_i\}. \tag{3}$$

The function $V(\Delta x)$ denotes the Optimal Velocity Function (OVF) determined by the inter-vehicle distance defined as

$$V(\Delta x) = \tanh(\Delta x - 2) + \tanh 2 \tag{4}$$

which was assumed monotonically increasing and bounded above function. The following characteristics are described by this OV model:

a. A car will maintain its maximum speed while maintaining a sufficient distance from the next car.

b. The optimal velocity of a car is determined by the distance to the next car.

The OV model was calibrated with respect to empirical data by Helbing and Tilch [6]. They adopted the following optimal function

$$V(\Delta x_i(t)) = V_1 + V_2 \tanh\left[C_1(\Delta x_i(t) - l_c) - C_2\right], \tag{5}$$

where l_c is considered as the length of the vehicle, that is chosen $5\,m$ in simulation. The values of parameters are $V_1 = 6.75\,ms^{-1}$, $V_2 = 7.91\,ms^{-1}$, $\kappa = 0.85\,s^{-1}$, $C_1 = 0.13\,m^{-1}$ and $C_2 = 1.57$. When compared to actual field data, it was shown that the OV model had problems with unrealistic deceleration and excessive acceleration. To address this issue, Helbing and Tilch [6] put forwarded a new model, called Generalized Force Model (GFM), as a solution as

$$\frac{dv_i(t)}{dt} = \kappa\{V(\Delta x_i(t)) - v_i\} + \lambda\,\Theta(-\Delta v)\,\Delta v, \tag{6}$$

where Θ is the Heaviside function. The Heaviside function is one when the velocity of the vehicle in front of it is lower than the velocity of the vehicle behind it; otherwise, it is zero.

The following vehicle will not brake even though its space headway is smaller than the safety distance if the leading vehicle is moving significantly quicker than the following one because the space headway between the two consecutive vehicles will grow. Observing the car-following event, Jiang et al. [7] claimed that the relative velocity between the following and the leading vehicles influenced the follower driver's behavior, therefore this factor should be considered explicitly. Based on the assumption, they presented a new model known as full velocity difference (FVD) model taking both negative and positive velocity difference into account in the following way

$$\frac{dv_i}{dt} = \kappa(V(\Delta x_i) - v_i) + \lambda \Delta v_i, \tag{7}$$

where $V(\Delta x_i)$ is the optimal velocity function and κ, λ are two reaction coefficients defined as

$$\kappa = 0.41 \quad \text{and} \quad \lambda = \begin{cases} 0.50 & \text{if } \Delta x_i \leq 100, \\ 0 & \text{otherwise.} \end{cases} \tag{8}$$

This model considered the impact of both the space headway and velocity difference. The model described above cannot be used to investigate the effects of the attribution of the driver on her/his driving behavior. In a real-world traffic system, different drivers exhibit different driving behaviors based on their attributions. Each driver has a different desired safety distance and optimal speed. Tang et al. [12] used the car-following model to account for driver attribution with the optimal speed defined as

$$V(\Delta x_i) = \begin{cases} v_{i-1}(t)\{1 + \tanh(C \times (\Delta x_i(t) - \Delta x_c(t)))\} \\ \qquad\qquad\qquad\qquad \text{if } \Delta x_i(t) < \Delta x_c(t), \\ v_{i-1}(t) + (v_{\max} - v_{i-1}(t)) \times \tanh(C(\Delta x_i(t) - \Delta x_c(t))) \\ \qquad\qquad\qquad\qquad \text{if } \Delta x_i(t) \geq \Delta x_c(t), \end{cases} \tag{9}$$

where C is the sensitivity coefficient which is related to the safety distance of the driver; $\Delta x_c(t)$ is an expected space headway that is related to the attribution of the driver; $v_{\max}$ represents the maximum speed of the vehicle. The expected headway was defined as

$$\Delta x_c(t) = v_i(t)\, t_w - \frac{(v_i(t))^2}{2a_{i,\min}} + \frac{(v_{i-1}(t))^2}{2a_{i-1,\min}} + h_{c,stop}, \tag{10}$$

where $h_{c,stop}$ is the driver reaction time while stopping the $(i-1)^{th}$ vehicle; $a_{i,min}$ is the maximum deceleration of i^{th} vehicle; $h_{c,stop}$ represents safety distance of the i^{th} vehicle between the i^{th} and $(i-1)^{th}$ vehicle while stopping the $(i-1)^{th}$ vehicle. If $v_{i-1}(t) >> v_i(t)$, $\Delta x_c(t) \leq h_{c,stop}$ or $\Delta x_c(t) < 0$ may be satisfied when the i^{th} vehicle stops, which is not realistic. To avoid this situation Tang et al. [12] defined the expected headway as

$$\Delta x_c(t) = \max\{h_{c,stop}, v_i(t)t_w - \frac{(v_i(t))^2}{2a_{i,\min}} + \frac{(v_{i-1}(t))^2}{2a_{i-1,\min}} + h_{c,stop}\}. \tag{11}$$

Because expected headway is important for driver attribution, each vehicle has its own headway. To present the drivers attribution Tang et al. [12] used the parameter r as follows:

a. $r < 0$ for the aggressive driver.

b. $r = 0$ for the neutral driver.

c. $r > 0$ for the conservative driver.

The driver's expected headway in terms of parameter r is defined as

$$\Delta x_c(t) = (1+r)\max\{h_{c,stop}, v_n(t)t_w - \frac{(v_i(t))^2}{2a_{i,\min}} + \frac{(v_{i-1}(t))^2}{2a_{i-1,\min}} + h_{c,stop}\}. \quad (12)$$

Considering the properties of the optimal velocity function as that was used in literature [1], Jiao et al. [9] explored the relation between the vehicle's space headway and optimal velocity, which was expressed as

$$S(\Delta x) = \frac{1}{1+e^{\Delta x_{safe} - \mu \Delta x}}, \quad (13)$$

where $S(\Delta x) \in [0,1]$ gives the sensitivity of optimal velocity to the space headway; Δx_{safe} represents the safety space headway; and μ is a parameter value in the interval $(0,1)$. $S(\Delta x)$ represents the sensitivity of the optimal velocity to the space headway for the different value of parameter μ. The optimal velocity also depends on the speed of the vehicle in front of it as well as on the distance between them. In order to better reflect the peculiarities of the drivers, Jiao et al. [9] proposed a new optimal velocity function, which is expressed as

$$V(\Delta x, v_{i-1}) = V_{\max}\left[S(\Delta x) - S(\Delta x_{safe})\right] - \left[1 - S(\Delta x)\right] v_{i-1}(t) \quad (14)$$

which satisfies the following conditions:

a. When $\Delta x = \Delta x_{safe}, V(\Delta x, v_{i-1}) \in [0, v_{i-1}(t)]$,

b. When $\Delta x = \Delta x_{safe}$ and $v_{i-1}(t) = 0, V(\Delta x, v_{i-1}) = 0$,

c. When Δx becomes larger, $V(\Delta x, v_{i-1}) \to V_{\max}$.

The dynamic equation so-called Reinforcement Car-following (RCF) model, which was described as

$$\frac{dv_i(t)}{dt} = \kappa\left[V(\Delta x, v_{i-1}) - v_i(t)\right] + \lambda\,\Delta v. \quad (15)$$

The following notes for equation (15) were provided as:

a. When the distance between the succeeding vehicles is close together, the velocity of the following vehicle is more dependent on the change in the velocity of the leading vehicle.

b. The effect of the velocity of a preceding vehicle on the speed of a following vehicle diminishes as the distance between successive vehicles grows.

c. When the distance between the succeeding vehicles approaches or exceeds the critical value's upper limit, the influence of the leader vehicle's velocity on the follower vehicle's velocity will vanish. In this situation, the velocity of the following vehicle is dependent only on the highest speed permitted on the road.

2.2. Car-following Model During Rainfall

Numerous environmental conditions, such as precipitation, snowfall, storms, etc., have significantly impacted the vehicle and the driver. Drivers modify their driving behavior to acclimate to the new surroundings. To study the impact of rainfall on the driving vehicles, we propose a dynamic equation by improving the previous models by introducing the rainfall-resisting force on the vehicle proportional to the velocity of the driving vehicle in the following way:

$$\frac{d(v_i(t))}{dt} = \kappa\,[V_{opt} - v_i(t)] + \lambda\,\Delta v - \gamma\, v_i(t), \tag{16}$$

where V_{opt} is optimal velocity function, λ represents a parameter value, Δv represents the velocity difference between the following and leading vehicles, and γ represents a parameter defined as function of t defined as

$$\gamma(t) = \begin{cases} \alpha\,(t - t_1)(t_2 - t) & \text{if } t_1 \leq t \leq t_2, \\ 0 & \text{otherwise}, \end{cases} \tag{17}$$

where α is some positive constant. It is assumed that the rainfall begins at time t_1 *seconds* and then the intensity of rainfall increases and has maximum intensity $\alpha(t_2 - t_1)^2/4$ at time $(t_1 + t_2)/2$ *seconds*. After having the maximum intensity, the intensity of rainfall begins to decrease and yields no impact as the rainfall stops at time t_2 *seconds*. Thus, the impact of rainfall is parabolic in nature in the time interval $t_1 \leq t \leq t_2$ and has no impact elsewhere.

One can experience that when s/he is driving the car at an increasing speed, s/he feels more obstacles from the weather conditions, like rainfall, snowfall, storm, etc. The impact increases as there is an increasing intensity of poor weather conditions.

3. Numerical Simulations and Results Discussion

Initially, assuming that a car-following platoon of eleven cars waiting uniformly with space headway $7.4\,m$ at a red traffic light signal at the intersection of the road with the optimal velocity of each vehicle is zero. When the traffic signal turns green, the time t begins, and the leading car immediately starts and accelerates at its maximum speed. The remaining other cars start gradually maintaining the safety distance between them. The impact of rainfall is simulated in the time interval $10 \leq t \leq 30$ *seconds*. The equation (16) is complex and can not be solved analytically. So, the Euler forward difference method is adopted to discretize the equation (16) into

$$v_i(t+\Delta t) = v_i(t) + \frac{dv_i(t)}{dt}\Delta t, \tag{18}$$

$$x_i(t+\Delta t) = x_i(t) + v_i(t)\Delta t + \frac{1}{2}\frac{dv_i(t)}{dt}(\Delta t)^2, \tag{19}$$

where $\Delta t = 0.001$ is the length of the time step. The study is carried out considering the normal behavior of the driver. The parameters $\lambda = 0.5$, $\Delta x_{safe} = 7.4\,m, \kappa = 0.41,\ v_{\max} = 14.66\,ms^{-1}$ are adopted from the literature [7], parameters $C = 0.05\,s$, $a_{i,\min} = -6\,ms^{-2},\ t_w = 0.8\,s$, $h_{c,stop} = 8.7\,m$ are adopted from the literature [12]. The other parameter $\mu = 0.07$ is adopted from the literature [9]. In the results of Figures 2 to 7, the red color is used to represent the dynamical behavior of the leading car. The green, black, yellow and magenta colors represent the dynamic behavior of the second, third, fourth and fifth cars, respectively. The remaining colors represent the dynamic behavior of the subsequent cars. We call Helbing's OV model as Model-I, Jiang's FVD model as Model-II, Tang's updated FVD model as Model-III and Jiao's RCF model as Model-IV. We use all these car-following models incorporating with our proposed dynamical equation during the rainfall and simulate to observe the impact of rainfall on the driving vehicles.

The subfigures presented in Figures 2 to 7 show the velocity, acceleration and spacing profiles of Model-I (subfigure (a)), Model-II (subfigure (b)), Model-III (subfigure (c)) and Model-IV (subfigure (d)). The subfigures in Figure 2 show the velocity profiles of car-following models without any impact of rainfall. The velocity of each car reaches the preset maximum speed $14.66\,ms^{-1}$ on $37, 35, 26$ and 26 *seconds* to Model-I, Model-II, Model-III and Model-IV, respectively.

The simulated results in Figure 3 depict how the eleven vehicles' speeds changed as the starting procedure progressed using different car-following models with the impact of rainfall. The velocities gained by leading car at $t = 10$

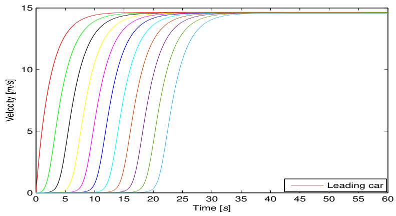

(a) Model-I

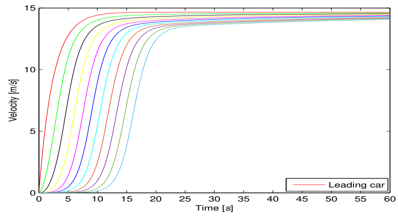

(b) Model-II

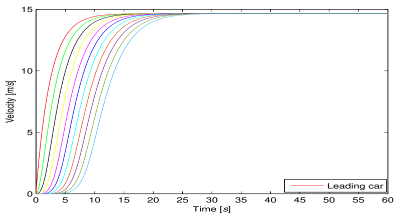

(c) Model-III

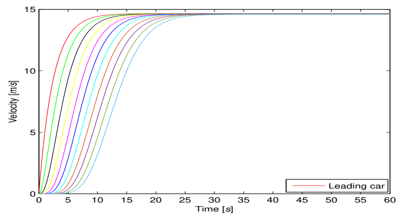

(d) Model-IV

Figure 2: Simulations of the velocities distributions of car-following models when the traffic signal turns green without the impact of rainfall.

seconds to Model-I, Model-II, Model-III and Model-IV are $14.66\,ms^{-1}, 14.4\,ms^{-1}$, $11.4\,ms^{-1}$ and $14.4\,ms^{-1}$ respectively. In the time interval $10 \leq t \leq 30$, due to the effect of γ, the velocity of each vehicle begins to decrease. The minimum velocities of the leading car to Model-I, Model-II, Model-III and Model-IV are $13.1\,ms^{-1}, 11.9\,ms^{-1}, 11.9\,ms^{-1}$ and $11.9\,ms^{-1}$ respectively which are gained at time 21, 22, 22.5 and 22 *seconds*. The minimum velocities of the last car to Model-I, Model-II, Model-III and Model-IV are $11.6\,ms^{-1}, 8.7\,ms^{-1}, 7.4\,ms^{-1}$ and $5.3\,ms^{-1}$ respectively which are gained at time 20, 20, 22.5 and 27 *seconds*. The velocities by leading car gained at $t = 30$ *seconds* to Model-I, Model-II, Model-III and Model-IV are $14.32\,ms^{-1}, 13.5\,ms^{-1}, 13.5\,ms^{-1}$ and $13.5\,ms^{-1}$ respectively. It is noticed that the minimum value of the last vehicle in Model-IV is the smallest among all the models due to the parameters they have considered. The velocity of each car reaches the preset maximum velocity $14.66\,ms^{-1}$ on $39, 46, 46$ and 46 *seconds* to Model-I, Model-II, Model-III and Model-IV, respectively.

The results in Figure 4 depict how the eleven vehicles' acceleration changed as the starting procedure progressed using different car-following models without the impact of rainfall. The acceleration of each car becomes stable at

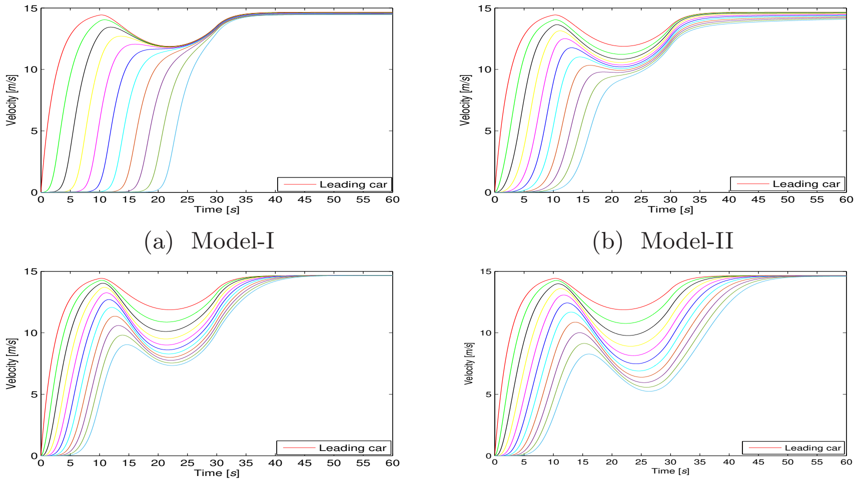

(a) Model-I (b) Model-II (c) Model-III (d) Model-IV

Figure 3: Simulations of the velocities distributions of car-following models when the traffic signal turns green with the impact of rainfall.

time $37, 26, 25,$ and 25 *seconds* to Model-I, Model-II, Model-III and Model-IV, respectively. The outcomes in Figure 5 show how the acceleration of the eleven vehicles changed as the starting operation advanced using various car-following models. The accelerations gained at $t = 10$ *seconds* to Model-I, Model-II, Model-III and Model-IV are $0\,ms^{-2}, 0.1\,ms^{-2}, 0.1\,ms^{-2}$ and $0.1\,ms^{-2}$ respectively. The maximum accelerations gained by the models are $12.4\,ms^{-2}$, $6\,ms^{-2}$, $6\,ms^{-2}$ and $6\,ms^{-2}$ respectively. The minimum accelerations gained in different models in the time interval $10 \leq t \leq 30$ are $0.3\,ms^{-2}$, $-0.46\,ms^{-2}$, $-0.74\,ms^{-2}$ and $-0.7\,ms^{-2}$ respectively. The accelerations gained by leading car at $t = 30$ *seconds* to the different models are $0.3\,ms^{-2}$, $-0.45\,ms^{-2}$, $0.1\,ms^{-2}$ and $0.1\,ms^{-2}$, respectively. The acceleration of each car becomes stable at time $39, 35, 45$ and 51 *seconds* to Model-I, Model-II, Model-III and Model-IV, respectively.

The simulated results in Figure 6 demonstrate how the headway difference between the consecutive vehicles changed as the starting procedure progressed using different car-following models without the impact of rainfall. It is observed that each vehicle of Model-III and Model-IV has almost constant spacing between the consecutive vehicle whenever each vehicle of Model-I and Model-II is constant but has different spacing.

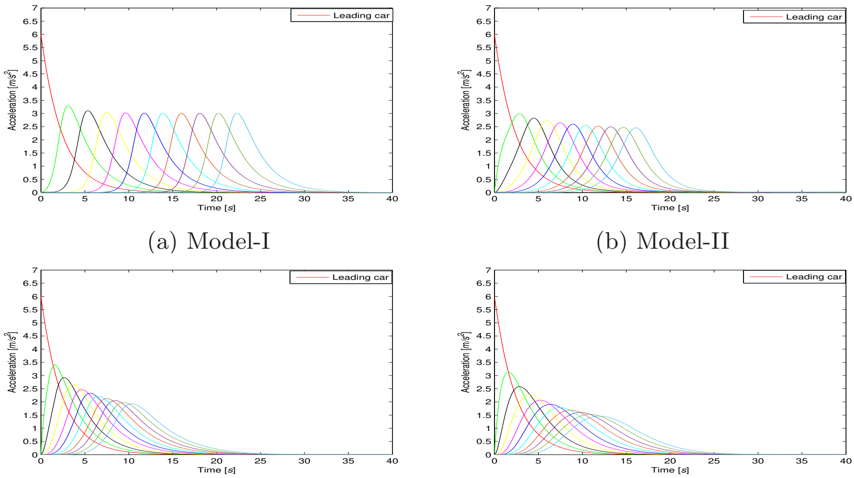

(a) Model-I (b) Model-II

(c) Model-III (d) Model-IV

Figure 4: Simulations of the acceleration distributions of car-following models when the traffic signal turns green without the impact of rainfall.

The results in Figure 7 demonstrate how the headway difference between the consecutive vehicles changed as the starting procedure progressed using different car-following models. At time $t = 10$ *seconds*, the spacing between first two cars in Model-I is $34\,m$ where as the difference between last two vehicles is $7.4\,m$. Similarly, the distance between first and second cars in Model-II, Model-III and Model-IV are $28.6\,m$, $21.5\,m$ and $38.5\,m$ respectively whereas the distance between last vehicles are $7.6\,m$, $12\,m$ and $11\,m$ respectively. At time $t = 30$ *seconds*, the spacing between first two cars in Model-I is $37\,m$ where as the difference between last two vehicles is $29.5\,m$. Similarly, the distance between first and second cars in Model-II, Model-III and Model-IV are $39.2\,m$, $36\,m$ and $38.5\,m$ respectively whereas the distance between last cars are $26\,m$, $22.5\,m$ and $24\,m$ respectively. It has been observed that each vehicle has almost constant spacing between the consecutive vehicle with different spacing in all models.

The simulated subfigures in Figure 8 show the averages of velocities, accelerations and spacing of all eleven vehicles of different car-following models with and without the impact of rainfall. Subfigure (a) shows the velocity behavior, subfigure (b) shows the acceleration behavior and subfigure (c) shows the spacing between the consecutive cars on a single-lane road. It is observed

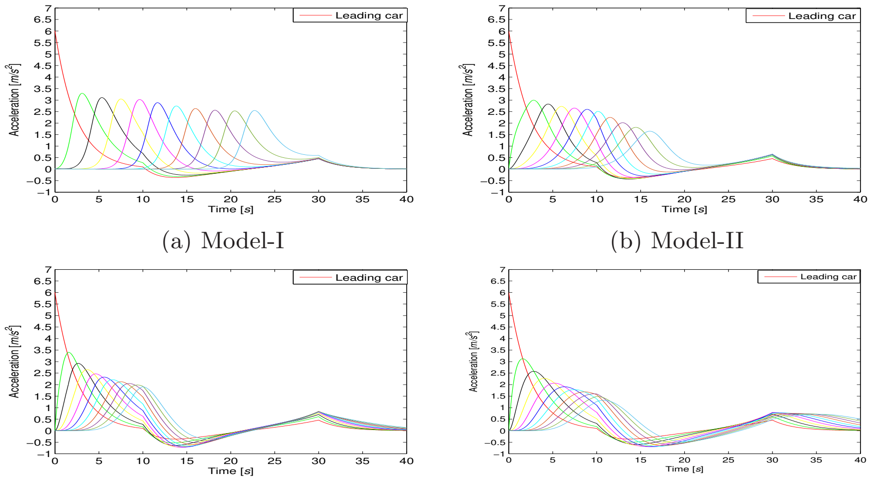

(a) Model-I (b) Model-II

(c) Model-III (d) Model-IV

Figure 5: Simulations of the acceleration distributions of car-following models when the traffic signal turns green with the impact of rainfall.

from the figure that the difference in average velocity is smaller in Model-I and higher in Model-IV in the time interval $10 \leq t \leq 30$. Similar behavior is observed in differences in average acceleration. But the average spacing between consecutive cars in Model-II is smaller and the Model-IV is larger among all the car-following models in the time interval $10 \leq t \leq 30$. It is also observed that all the models have a different time to be stable for velocity, acceleration and spacing behavior due to the impact of rainfall.

4. Conclusion

The dynamic behavior of the traffic model can be affected by many factors. The optimal velocity function, space headway, velocity of the preceding vehicle and driver sensitivity play a significant role in the microscopic car-following model. Similarly, the vehicle and the driver are significantly impacted by several environmental factors such as rainfall, snowfall, storm, etc. In such circumstances, vehicles reduce their speed and widen their following distance, delaying traffic and lengthening travel times. The speed-density functions that represent the process of continuous traffic flow are changing as a result of the speed reduc-

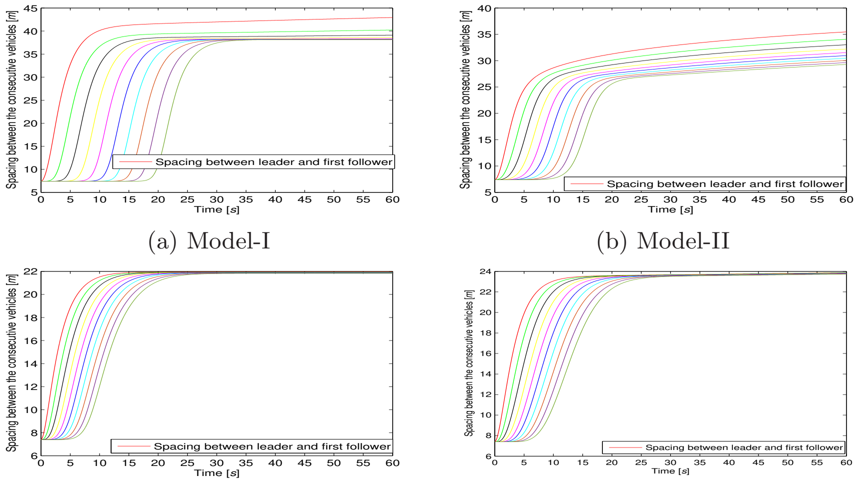

(a) Model-I (b) Model-II

(c) Model-III (d) Model-IV

Figure 6: Simulations of the spacing between consecutive vehicles of the different models, starting when the traffic signal turns green without the impact of rainfall.

tion and the stable-unstable domain is shifting. The numerical results of the proposed dynamic equation of the car-following model show the impact of rainfall on the dynamical behaviors of different car-following models in the given time interval. The results obtained from the proposed model seem in the best agreement with the real-world problem.

Acknowledgments

We would like to acknowledge University Grants Commission Nepal for providing the research support. We are also thankful to the reviewers for their constructive comments and suggestions which indeed improved the quality of the article very well.

References

[1] M. Bando, K. Hasebe, A. Nakayama, A. Shibata and Y. Sugiyama, Dynamical model of traffic congestion and numerical simulation, *Phys. Rev. E*, **51**, No 2 (1995), 1035-1042.

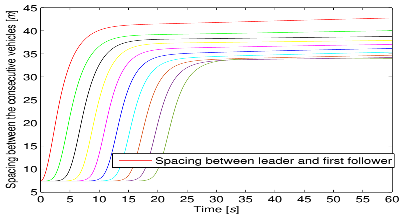

(a) Model-I

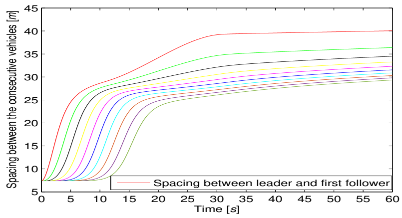

(b) Model-II

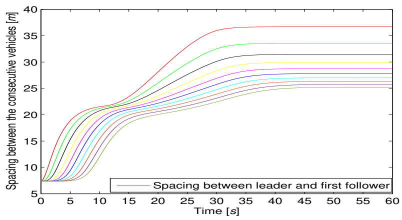

(c) Model-III

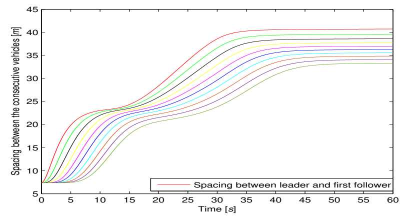

(d) Model-IV

Figure 7: Simulations of the spacing between consecutive vehicles of the different car-following models, starting when the traffic signal turns green with the impact of rainfall.

[2] S. Di-hua, L.I. Yong-fu and T. Chuan, Car-following model based on the information of multiple ahead and velocity difference, *Syst. Eng. Theory Prac.*, **30**, No 7 (2010), 1326-1332.

[3] H.X. Ge, R.J. Cheng and Z.P. Li, Two velocity difference model for a car-following theory, *Phys. A Stat. Mech. Its Application*, **387**, No 21 (2008), 5239-5245.

[4] H.X. Ge, S.Q. Dai, L.Y. Dong and Y. Xue, Stabilization effect of traffic flow in an extended car-following model based on an intelligent transportation system application, *Phys. Rev. E, Stat. Nonlinear Soft Matter Phys.*, **70** (2004), 066134:1-066140:4.

[5] H. Gong, H. Liu and B.H. Wang, An asymmetric full velocity difference car-following model, *Phys. A Stat. Mech. Its Application*, **387**, No 11 (2008), 2595-2602.

[6] D. Helbing and B Tilch, Generalized force model of traffic dynamics, *Phys. Rev. E*, **58**, No 1 (1998), 133-138; doi.10.1103/PhysRevE.58.133.

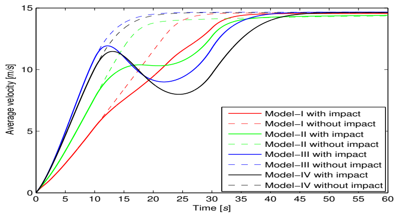

(a) Comparision of average velocity

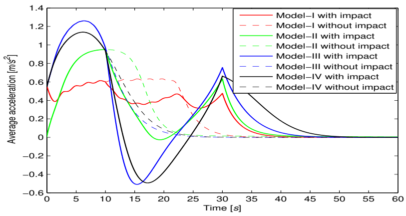

(b) Comparison of average acceleration

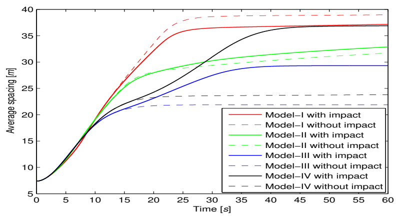

(c) Comparison of average spacing

Figure 8: Comparison of the dynamical behavior of car-following models from the traffic signal.

[7] R. Jiang, Q.S. Wu and Z.J. Zhu, Full velocity difference model for a car-following theory, *Phys. Rev. E*, **64**, No 1 (2001), 017101:1-017101:4.

[8] S. Jiao, S. Zhang, Z. Li, B. Zhou and D. Zhao, An improved car-following speed model considering speed of the lead vehicle, vehicle spacing, and driver's sensitivity to them, *J. Adv. Transp.*, **2020** (2020), 2797420:1-2797420:13; doi.10.1155/2020/2797420.

[9] S. Jiao, S. Zhang, B. Zhou, Z. Zhang and L. Xue, An extended car-following model considering the driver's characteristics under a V2V communication environment, *Sustainability*, **12**, No 4 (2020), 1552; https://doi.org/10.3390/su12041552.

[10] M. Klawtanong, S. Limkumnerd, Dissipation of traffic congestion using autonomous-based car-following model with modified optimal velocity, *Phys. A Stat. Mech. Its Appl.* **542** (2020), 123412:1-123412:9.

[11] L.A. Pipes, An operational analysis of traffic dynamics, *J. of App. Phys.*, **24**, No 3 (1953), 274-281.

[12] T.Q. Tang, J. He, S.C. Yanga and H.Y. Shang, A car-following model accounting for the driver attribution, *Physica A*, **413** (2014), 583-591.

[13] T.Q. Tang, J.G. Li, H.J. Huang and X.B. Yang, A car-following model with real-time road conditions and numerical tests, *Measurement*, **48** (2014), 63-76.

[14] T.Q. Tang, W. Shi, H.Y. Shang and Y. Wang, A new car-following model with consideration of inter-vehicle communication, *Nonlinear Dynam.*, **76** (2014), 2017-2023.

[15] T.Q. Tang, Y. Wang, X. Yang and Y. Wu, A new car-following model accounting for varying road condition, *Nonlinear Dynam.*, **70** (2012), 1397-1405.

[16] W. Tao, G.Z. You and Z. Xiao-Mei, Multiple velocity difference model and its stability analysis, *Acta Phys. Sin.*, **55** (2006), 634-638.

[17] R.E. Wilson, An analysis of Gipps's car-following model of highway traffic, *IMA J. Appl. Math.*, **66**, No 5 (2001), 509-537; doi.10.1093/imamat/66.5.509.

[18] D.F. Xie, Z.Y. Zhao and X. Gao, Stabilization of traffic flow based on the multiple information of preceding cars, *Commun. Comput. Phys.*, **3**, No 4 (2008), 899-912.